Available online at www.sciencedirect.com
ScienceDirect
Catalysis Today 133–135 (2008) 192–199
CATALYSIS TODAY
www.elsevier.com/locate/cattod

Environmentally friendly synthesis of Wells–Dawson heteropolyacids Active acid sites investigation through TPSR of isopropanol

Silvana R. Matkovic, Graciela M. Valle, Luis A. Gambaro, Laura E. Briand *

Centro de Investigación y Desarrollo en Ciencias Aplicadas, Dr. J.J. Ronco, CONICET, Universidad Nacional de La Plata,
Calle 47 No 257, B1900AJK La Plata, Buenos Aires, Argentina

Abstract

Fosfo-tungstic and fosfo-molybdic Wells–Dawson heteropolyacids, $H_6P_2W_{18}O_{62}\cdot xH_2O$ and $H_6P_2Mo_{18}O_{62}\cdot xH_2O$ respectively, were synthesized through ion-exchange. This novel method possesses a higher yield (~90%) than the conventional organic route (~70%).

Wells–Dawson heteropolyacids are obtained when the corresponding ammonium salt [$(NH_4)_6P_2W_{18}O_{62}\cdot 13H_2O$ or $(NH_4)_6P_2Mo_{18}O_{62}\cdot 12H_2O$] is kept in contact with an acid resin [about (1:0.8) salt:resin weight ratio] up to 3 days. The use of an organic media instead of an aqueous media greatly favors the completeness of the exchange.

Temperature programmed surface reaction of chemisorbed isopropoxy species towards propylene allows determined the number of active acid surface/bulk sites and the activation energy of the surface reaction. This parameter provided evidences of the influence of the central phosphorous atom and oxide supports on the acid strength of the active sites.

Keywords: HPA; Wells–Dawson; Keggin; POM; Active sites; Molecular probe

1. Introduction

Heteropolyanions $[X_yM_xO_m]^{n-}$ are composed by a close-packed framework of metal–oxygen octahedrons, M–O ($M = Mo^{6+}$, W^{6+}, V^{5+}) surrounding a central atom, X (Si^{4+}, P^{5+}, etc.) [1]. Nowadays, many research efforts are devoted to investigate both Keggin $[XM_{12}O_{40}]^{3-}$ and Wells–Dawson-type $[X_2M_{18}O_{62}]^{6-}$ anions due to their promising application as catalytic materials [2,3]. The free acid form of the heteropolyanions, i.e. Keggin $H_3XM_{12}O_{40}$ and Wells–Dawson $H_8X_2M_{18}O_{62}$ type compounds, are solid super-acids since their acid strength is greater than 100% H_2SO_4. Therefore, many heteropolyacids are more active catalysts than conventional organic and inorganic acids in liquid-phase reaction. The insolubility of the heteropolyacids in many liquid organic substances allows an easy separation and reutilization of these catalysts [3,4].

Undoubtedly, the catalytic processes based on heteropolyacids are an outstanding contribution in the development of environmental benign technologies. However, the synthesis of these compounds is rather complicated, involves the use of dangerous chemicals and produces harmful liquid and gaseous wastes.

Fosfo-tungstic $H_6P_2W_{18}O_{62}\cdot 24H_2O$, fosfo-molybdic $H_6P_2Mo_{18}O_{62}\cdot nH_2O$ ($n = 33$–37) and arsenic-molybdic $H_6As_2Mo_{18}O_{62}\cdot nH_2O$ ($n = 25$–35) Wells–Dawson acids have been synthesized. The heteropolyacids are synthesized through the ‘‘etherate method’’, electrodialysis, ion-exchange and precipitation with sulfuric acid [5].

The ‘‘etherate method’’ requires a strongly acidified aqueous solution of the heteropolyanion (from an aqueous soluble heteropolysalt) that is shaken with diethyl ether in order to separate three phases: an upper ether layer, an aqueous layer and a heavy oily layer. This layer contains an etherate of the heteropolyacid which nature is unknown. The etherate is decomposed with water and the solution is evaporated until the acid crystallizes. According to early studies by Wu and our own experience, this method does not yield pure $H_6P_2Mo_{18}O_{62}\cdot nH_2O$ but a mixture with fosfo-molybdic Keggin-type acid $H_3PMo_{12}O_{40}$ [6].

This technique requires expensive and dangerous chemicals, possesses a low yield towards the acid, produces an important

---

* Corresponding author.
E-mail address: briand@quimica.unlp.edu.ar (L.E. Briand).

0920-5861/$ – see front matter © 2008 Elsevier B.V. All rights reserved.
doi:10.1016/j.cattod.2007.12.120

amount of harmful wastes (concentrated HCl and ether mixture) and is time consuming.

Kozhevnikov et al. applied electrodialysis to synthesize iso- and heteropolyacids of various structures in highly concentrated aqueous solutions [7]. In general, this method avoids the use of diethyl ether and inorganic acids since the solutions are electrochemically acidified during operation. However, the synthesis of the $H_6P_2W_{18}O_{62}$ is rather complicated since requires the electrodialysis of a mixture of H_3PO_4 and Na_2WO_4 up to a certain pH value, then a thermal treatment (6 h at 423 K) and dialysis again to obtain the desired product.

More recently, Wijesekera et al. patented the synthesis of fosfo-molybdic Wells–Dawson-type polyoxometallates through an ion-exchange methodology in aqueous media [8,9]. Although infrared spectroscopy and nuclear magnetic resonance were applied to establish the purity of the compounds, no investigation of the surface properties was performed. Moreover, the ion-exchange in organic media should also be explored since molybdenum based heteropoly compounds are unstable in aqueous solution [10].

The present investigation describes a detailed examination of the conditions (solvents, substrate–resin ratio and time of the exchange) to optimize the synthesis of fosfo-tungstic and fosfo-molybdic Wells–Dawson acids through the ion-exchange method. Additionally, isopropanol chemisorption and temperature programmed surface reaction was used as a probe to investigate the number of active acid sites and the activation energy in order to compare the acid properties of HPAs with various catalytic materials.

2. Experimental

2.1. Synthesis of the $(NH_4)_6P_2W_{18}O_{62}\cdot 13H_2O$ and $(NH_4)_6P_2Mo_{18}O_{62}\cdot 12H_2O$ salts

The heteropoly acids were synthesized through the ion-exchange of the fosfo-tungstic $(NH_4)_6P_2W_{18}O_{62}\cdot 13H_2O$ and fosfo-molybdic $(NH_4)_6P_2Mo_{18}O_{62}\cdot 12H_2O$ Wells–Dawson ammonium salts. The salts were synthesized according to methods reported in the literature [10,11].

Additionally, the fosfo-tungstic Wells–Dawson acid $H_6P_2W_{18}O_{62}$ was synthesized according to the ‘‘etherate method’’ with a 71.4% yield. The details of the synthesis have been published previously [12].

2.2. Ion-exchange method

A Dowex HCR-W2 (Sigma–Aldrich) acid resin was used in the ion-exchange experiments. This material possesses a 1.9 mequiv./ml exchange capacity according to the vendor. The density of the wet resin was determined as 1.18 g/ml which results in a 2.4 mequiv./g exchange capacity. According to these data, the stoichiometric exchange ratios would be (1:0.6) and (1:0.8) salt:resin weight ratio for the $(NH_4)_6P_2W_{18}O_{62}\cdot 13H_2O$ (MW. 4708 g/mol, 6×10^{-3} mequiv./mol) and $(NH_4)_6P_2Mo_{18}O_{62}\cdot 12H_2O$ (MW. 3106 g/mol, 6×10^{-3} mequiv./mol) salts, respectively.

The ion-exchange experiments were performed both in a column and batchwise. The flow rate of the effluent in the column experiments was calculated as the ratio between the volume of effluent collected per unit of time and volume of wet resin.

The starting ammonium salts were dissolved in absolute ethanol (Merck, 99.8%), distilled water or a 50:50 ethanol–water mixture prior to the contact with the resin. The resultant solution after the exchange was allowed to dry at room temperature prior to the infrared analysis.

2.3. Supported catalysts and additional materials

The fosfo-tungstic acid was supported on ZrO_2 (Degussa fumed zirconia), TiO_2 (Degussa P-28) and SiO_2 (EH-5 Cab-O-Sil) at the theoretical monolayer coverage. The loading was calculated considering that the acid would cover 157 Å^2 per anion. However, specific surface area measurement demonstrated that the amount of acid that is suitable to be well dispersed on silica is considerably below the theoretical monolayer coverage. A percentage above 9% greatly diminishes the surface area of the support.

Supported catalysts were synthesized through conventional incipient wetness in aqueous media. The catalysts were dried at room temperature overnight and further calcined at 573 K for 4 h.

The acidity of the HPAs and several tungsten and molybdenum based materials such as, bulk tungsten trioxide, monolayer supported tungsten species, nano-particulate mesoporous tungsten–zirconium oxide and Keggin type heteropolyacids was compared.

Bulk WO_3 was obtained through the thermal decomposition of $(NH_4)_6H_2W_{12}O_{40}$ (Fluka A.G.) at 1073 K for 4 h. Monolayer supported tungsten species over oxide supports (8% WO_3/TiO_2 and 6% WO_3/ZrO_2) were synthesized through incipient-wetness impregnation and were kindly provided by Lehigh University (PA, USA) [13].

The mesoporous 30% WO_3/ZrO_2 nanoparticles (~5 nm) were provided by Rice University (TX, USA). The details of the synthesis procedure are reported in the literature [14].

Commercial fosfo-tungstic $H_3PW_{12}O_{40}\cdot xH_2O$ (Fluka puriss.) and fosfo-molybdic $H_3PMo_{12}O_{40}\cdot xH_2O$ acids (Sigma–Aldrich) were used.

2.4. Characterization techniques

2.4.1. Infrared spectroscopy

The presence of the ammonium ion after the exchange and the stability of the Wells–Dawson structure were followed through infrared spectroscopy. The analysis was performed with a FTIR Bruker IFS 66 equipment under ambient conditions. The solid samples were diluted with KBr and pressed into thin wafers.

2.4.2. Gravimetric and differential thermal analyses (TGA–DTA)

TGA–DTA analyses were performed in a Shimadzu TGA-50H and DTA-50 equipments, respectively. The samples were heated at 10 K/min in a stream of helium (40 sccm) from room temperature to 1073 K. Typically, 100 mg of the sample placed in a platinum cell was used for both analyses.

2.4.3. Nuclear magnetic resonance ^{31}P NMR

The purity of the Wells–Dawson structure was followed through nuclear magnetic resonance of phosphorous. Liquid NMR spectra were performed with a Bruker AM 500 spectrograph both in D_2O and deutered methanol CD_3OD under ambient conditions. The equipment operates at a frequency of 202.458 MHz with 11.3 μs pulses. The analysis involved 8–800 pulse responses with a resolution of 0.25 Hz per point.

2.4.4. Specific surface area and pore volume determination

The adsorption–desorption isotherms of N_2 at 77 K were determined with a Micromeritics Accusorb 2020 surface area and porosity analyzer. The samples were degassed at 373 K under vaccum until a pressure of 10^{-3} Torr was reached. The specific surface area and pore diameter were determined with the BET and *t*-plot methods, respectively.

2.4.5. Chemisorption and temperature programmed surface reaction spectroscopy

The number and properties of the active sites were determined by adsorption of isopropanol at room temperature followed by temperature programmed surface reaction (TPSR). Typically, 20–90 mg of the sample is used during the experiments. The sample is pretreated at 673 K (373 K for $H_6P_2Mo_{18}O_{62}\cdot xH_2O$) for 1 h under a flow of pure oxygen prior to chemisorption and TPSR analysis. Then is allowed to cool down to the adsorption temperature under a flow of helium (35 cm^3(NTP) min^{-1}). Successive pulses of 0.5 μl of isopropanol (Merck P.A., 100%) are dosed through a heated septum until the saturation of the heteropolyacid is reached. The adsorption process is monitored *in situ* through a mass spectrometer and a conductivity cell that detects the non-adsorbed alcohol and/or the species desorbed from the sample. After the saturation, the sample is heated up to 723 K at 10 K/min for the temperature programmed surface reaction experiment. The species resulting of the reaction of the surface species are detected in the mass spectrometer and recorded in a computer. The following *m*/*e* ratios were employed to identify the desorbed species: C_5H_7OH, $m/e = 45$; C_3H_6, $m/e = 41$; diisopropyl ether, $m/e = 31$ and 87; acetone, $m/e = 43$ and 58; H_2O, $m/e = 18$; CO_2, $m/e = 44$ and CO, $m/e = 28$. The details of the calibration procedures of isopropanol and propylene were published before [15].

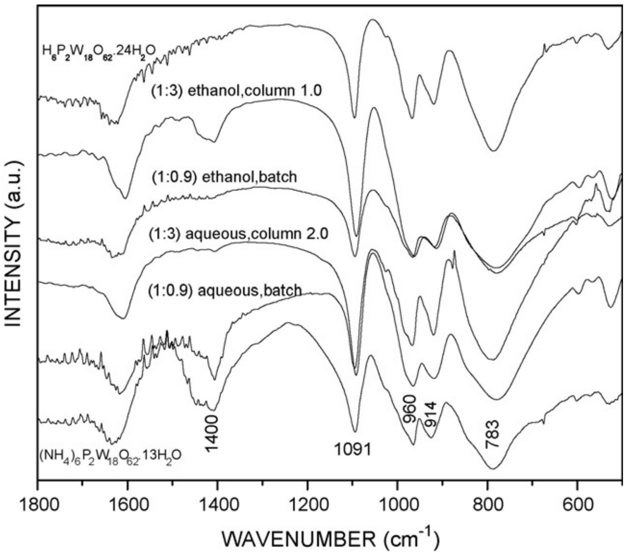

Fig. 1. Infrared spectra of the $(NH_4)_6P_2W_{18}O_{62}\cdot 13H_2O$ salt, the $H_6P_2W_{18}O_{62}\cdot 24H_2O$ heteropolyacid obtained through the conventional organic method and the materials obtained through the ion-exchange of the salt in a column containing (1:3) salt:resin weight ratio (1.0 and 2.0 min^{-1} indicates the flow rate of the effluent), and 3 days in batch with a (1:0.9) ratio, both in aqueous and organic media.

Temperature programmed desorption analysis were also performed over the heteropolyacids without previous thermal treatments in order to identify the temperature of desorption of water and ethanol ($m/e = 31$ and 46) that remain adsorbed after the ion-exchange.

3. Results and discussion

3.1. Operative conditions for the synthesis of heteropolyacids through ion-exchange

The influence of the operation conditions such as, amount of resin (salt:resin weight ratio), nature of the solvent, temperature and time in the exchange of ammonium by protons ions was investigated in batch experiments. A great variety of conditions were tested however, only the most representative results are included in order to simplify the discussion.

Fig. 1 shows the infrared spectra of the materials obtained through the ion-exchange of the fosfo-tungstic salt with the acid resin performed in aqueous and ethanol media both in batch and column. Additionally, the spectrum of the fosfo-tungstic Wells–Dawson acid $H_6P_2W_{18}O_{62}\cdot 24H_2O$ synthesized through the ‘‘etherate method’’ and the starting ammonium fosfo-tungstic Wells–Dawson salt $(NH_4)_6P_2W_{18}O_{62}\cdot 13H_2O$ salt are presented for comparison.

The spectrum of the fosfo-tungstic Wells–Dawson acid possesses an intense band at 1091 cm^{-1} assigned to the stretching mode of the P–O species that is considered a fingerprint of the Wells–Dawson heteropolyanion $P_2W_{18}O_{62}{}^{6-}$ structure. The bands at 960, 914 and 783 cm^{-1} corresponds to the W–O species of the cage structure surrounding the central phosphorous species [12]. The spectra of the materials after being in contact with the acid resin in aqueous media possess a band at 1400 cm^{-1} that corresponds to $NH_4{}^+$ species indicating that the exchange was not complete even after 3 days.

In contrast, the organic media favors the ion-exchange based on the observation that the pure fosfo-tungstic heteropolyacid is obtained after 3 days in contact with (1:0.9) salt:resin weight ratio. Further experiments demonstrated that contact times and salt:resin ratios below 3 days and (1:0.9) do not yield the acid.

Additionally, the ion-exchange was carried in a glass column with a (1:3) salt:resin weight ratio. The experiments were performed at varying flow rates (0.8–3.6 BV/min) due to the fact that this parameter was difficult to reproduce from one experiment to another. This is a typical drawback of the exchange columns that possesses a regular two-ways stopcock. In contrast with the results obtained batchwise, the exchange of the fosfo-tungstic salt was complete when the experiment was carried in aqueous medium but not in ethanol.

Surprisingly, the yield of the synthesis was 95.5%, which results higher than the ‘‘etherate’’ route for the fosfo-tungstic acid (see Section 2.1).

^{31}P NMR analysis was not useful to determine the effectiveness of the exchange since both the starting ammonium fosfo-tungstic Wells–Dawson salt and the acid possesses similar signals at -10.78, -11.55 and -12.28 ppm which makes difficult to distinguish both substances (spectra not shown).

The experiments with the ammonium fosfo-molybdic salt with various salt:resin weight ratios demonstrated that a complete exchange is achieved with the stoichiometric (1:0.8) salt:resin exchange ratio. Again, the comparison of the infrared spectra of the materials obtained in aqueous (spectra not shown) and organic media indicate that the ion-exchange is greatly favored in organic media.

Fig. 2 shows the effect of time and temperature in the ion-exchange of the ammonium fosfo-molybdic Wells–Dawson salt in organic media (ethanol and a 50:50 ethanol:water mixture). The spectra of the material obtained after 6 and 24 h of ion-exchange in ethanol and after 3 days in ethanol:water mixture possess the characteristic signals of the starting Wells–Dawson salt $(NH_4)_6P_2Mo_{18}O_{62}\cdot 12H_2O$. The fosfo-molybdic Wells–Dawson structure presents the infrared signal of the central phosphorous species at 1078 and 904 cm^{-1}, and Mo–O species at ~936 and 769 cm^{-1} [10,16]. Additionally, the ammonium salt possesses the infrared signal of the NH_4^+ species at 1403 cm^{-1} similarly to the fosfo-tungstic salt.

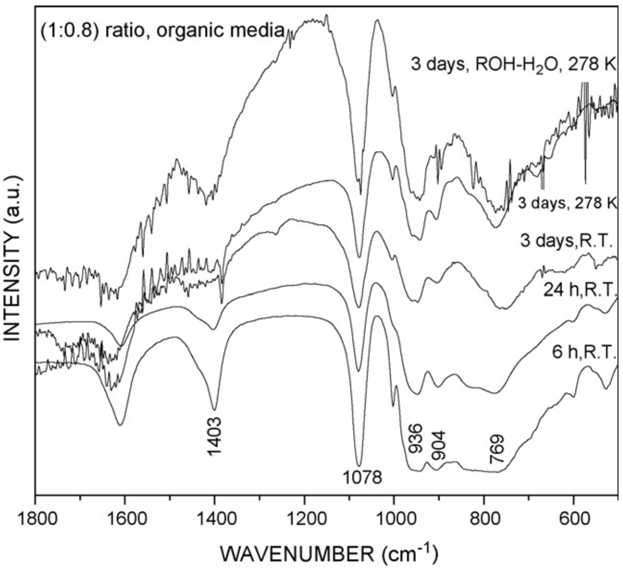

Fig. 2. Infrared spectra of the $(NH_4)_6P_2Mo_{18}O_{62}\cdot 12H_2O$ salt and the materials obtained through the ion-exchange of the salt in contact with (1:0.8) salt:resin weight ratio and variable time and temperature of exchange in ethanol and ethanol:water media.

The fosfo-molybdic acid $H_6P_2Mo_{18}O_{62}\cdot 27H_2O$ is obtained after 3 days of ion-exchange with a 92.2% yield. Similar results were obtained either at room temperature or below which, clearly demonstrated that low temperatures do not favors the exchange in contrasts with the technique reported by Wijesekera et al. [8,9].

Further studies through ^{31}P NMR were performed in order to establish the purity of the fosfo-molybdic acid obtained through ion-exchange. Fig. 3 shows that the ammonium fosfo-molybdic Wells–Dawson salt possesses a single signal at about -1.61 ppm in deutered methanol [10,16]. The spectrum of the salt partially exchanged shows signals at -1.67 ppm (-2.42 ppm in D_2O) assigned to the fosfo-molybdic Wells–Dawson acid along with the characteristic signal of the of the Keggin $PMo_{12}O_{40}^{3-}$ species at -3.64 ppm (-3.99 ppm in D_2O) [17]. A third one, at -2.10 ppm could not be identified. However, might be attributed to an interaction with the organic solvent since is not observed in deutered water.

Previous studies demonstrated that the fosfo-molybdic Wells–Dawson salt $(NH_4)_6P_2Mo_{18}O_{62}$ decomposes in the lacunar Keggin-type anion $H_xPMo_{11}O_{39}^{(7-x)-}$ in aqueous media [10]. Nevertheless, the degradation of the structure is avoided in organic solvents such as, alcohols [16]. The observation that traces of Keggin species appear in the analysis performed in CD_3OD along with the acid obtained in organic media (without the presence of non-exchanged salt), unambiguously demonstrate that those species are produced due to the decomposition of the acid. Further degradation of the fosfo-molybdic Keggin anion towards the lacunar species is avoided due to the highly acid medium [17].

3.2. *Thermal stability of Wells–Dawson heteropolyacids*

Temperature programmed desorption analysis gave insights on the species evolved upon heating of the heteropolyacids that were synthesized through ion-exchange using ethanol as solvent. Figs. 4 and 5 show the distribution of substances produced during the temperature programmed desorption analysis of the acids (without previous thermal treatments).

The fosfo-molybdic acid presents two intense signals due to water loss centered at 403 K and 543 K. Complementary thermo-gravimetric analysis revealed that 24 and 3 water moles per mol of acid are released consecutively.

The TPD analysis demonstrated that ethanol strongly interacts with the heteropolyanion structure since desorbs as CO/CO_2 above 600 K. No molecular desorption is observed during the analysis (see the *m*/e = 31 signal) which suggests that the alcohol is chemisorbed within the structure.

Further, infrared analyses of the heteropolyacid after calcination at various temperatures demonstrated that the Wells–Dawson structure maintains intact during the first dehydration process and begins a structural rearrangement towards a Keggin structure at 473 K (spectra not shown). Only the signals belonging to the $PMo_{12}O_{40}^{3-}$ anion at 1065 cm^{-1}

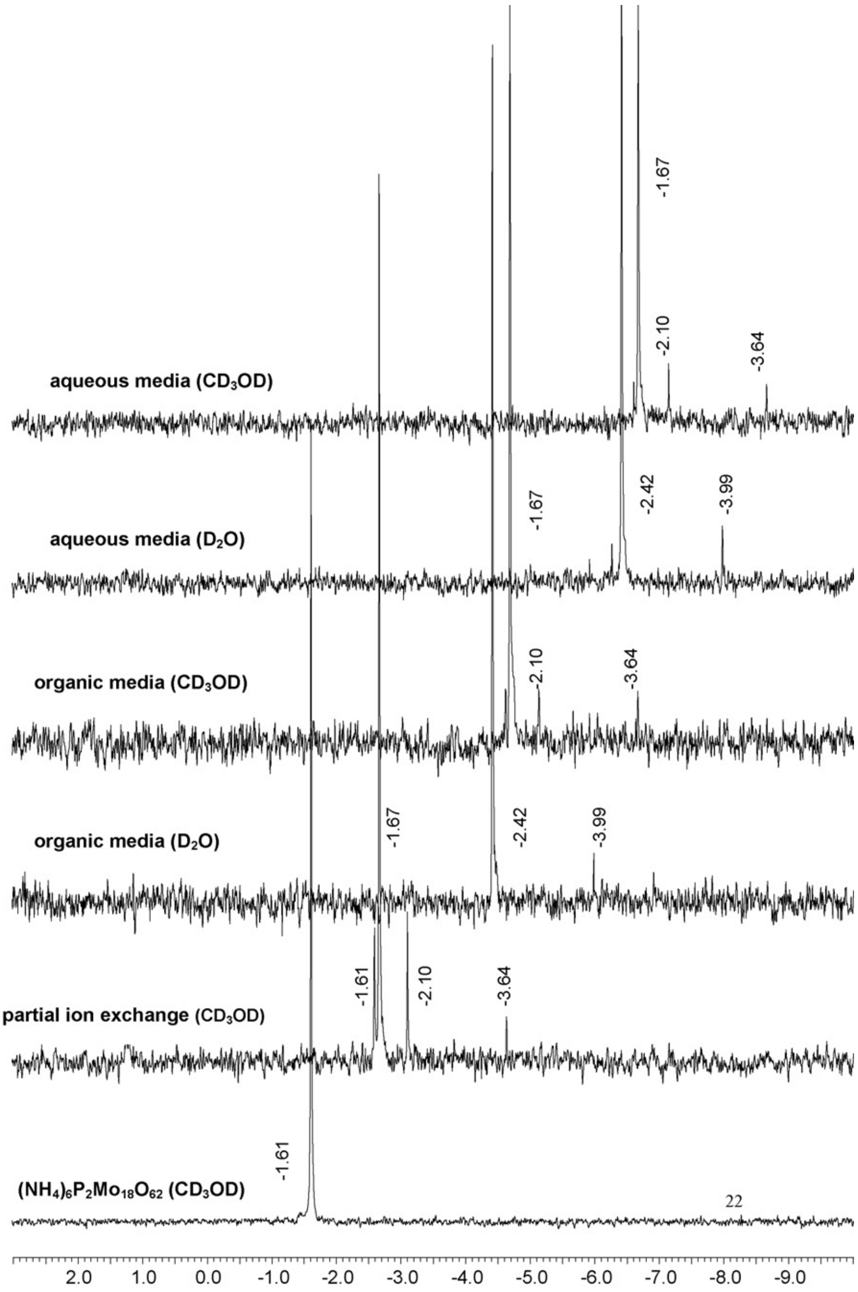

Fig. 3. ^{31}P nuclear magnetic resonance spectra of pure ammonium fosfo-molybdic Wells–Dawson salt and after being partially and completely exchanged with the acid resin in aqueous and organic media. The spectra were taken both in deutered water (D_2O) and methanol (CD_3OD).

(P–O species) and 960 cm^{-1} (Mo–O species) were observed at 523 K indicating that the Wells–Dawson structure was completely degraded to a Keggin type structure [17]. The infrared signals at 569, 871 and 994 cm^{-1} indicate that the heteropolyanion collapses completely towards MoO_3 at 873 K.

The fosfo-tungstic acid also shows a broad signal due to water loss from room temperature to 553 K and a smaller one centered at 523 K (see Fig. 5). These observations are in agreement with the consecutive loss of water of crystallization associated with the protons as $H^+(H_2O)_n$, H_3O^+ and $H_5O_2^+$ species reported in the literature [12,18]. Although, no molecular desorption of ethanol was observed, the alcohol decomposed to CO at a much lower temperature than the fosfo-molybdic counterpart (408 K vs. 694 K). Further infrared analysis demonstrated that the structure was unaltered after de TPD process (spectra not shown).

Interestingly, both materials showed a continuous desorption of molecular oxygen ($m/e = 32$) indicating that are reduced during the thermal treatment. This behavior that has not been reported in the literature before, might explain the typical change of color observed after calcination of HPAs and clearly indicates that any thermal treatment of these materials should be carried under oxygen atmosphere to avoid the modification of the surface.

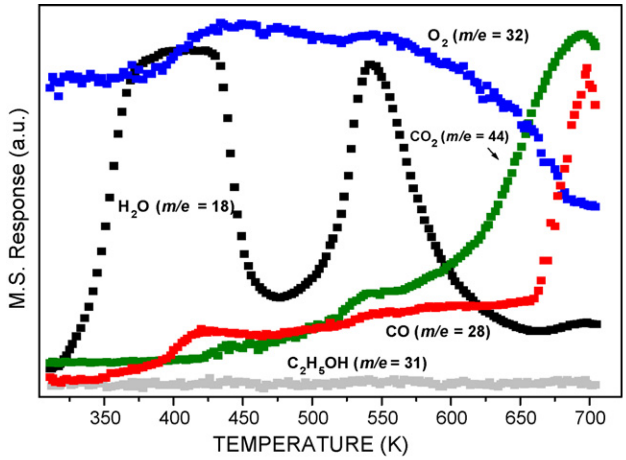

Fig. 4. Temperature programmed desorption spectra of $H_6P_2Mo_{18}O_{62}\cdot 27H_2O$.

3.3. Insights on the acid properties of Wells–Dawson HPAs through molecular probes: comparison with various catalytic materials

3.3.1. Number and nature of accessible active acid sites

Isopropanol was used as a probe molecule to characterize the acidity of heteropolyacid compounds since the products distribution upon reaction depends on the nature of the surface active sites. Strong Brönsted (H^+) and Lewis acid sites catalyze the dehydration of isopropanol to propylene (di-isopropyl ether over weak Lewis acid sites) and redox/basic sites lead to the dehydrogenation of the alcohol to acetone.

Previous investigations demonstrated for the first time in the literature that *in situ* chemisorption and quantitative temperature programmed surface reaction of isopropanol is a valuable tool to determine the nature, number and acid strength of the surface and/or bulk active sites of tungsten oxide based catalysts and particularly of the heteropolycompounds [15].

The chemisorption of isopropanol at 313 K leads to the coverage of the heteropolyacids with a stable monolayer of adsorbed isopropoxy species and avoids further surface reaction. These adsorbed intermediate-reactive alkoxy species further react and desorb as propylene (or other product depending on the nature of the site) upon controlled heating during the TPSR experiment. Therefore, the quantification of the desorbed product is proportional to the number of active sites on isopropanol dehydration.

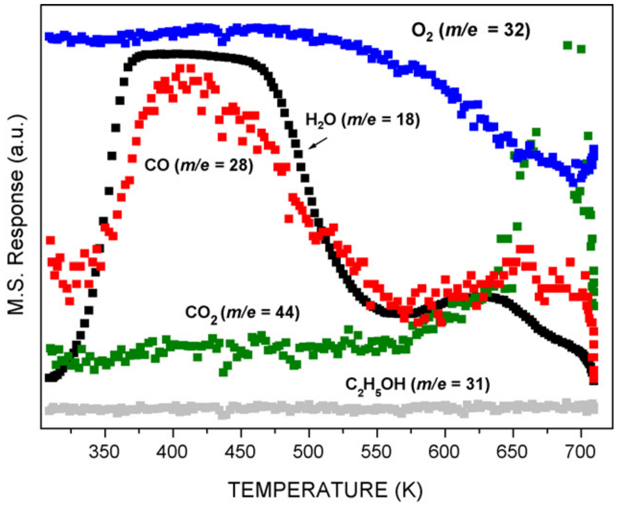

Fig. 5. Temperature programmed desorption spectra of $H_6P_2W_{18}O_{62}\cdot xH_2O$.

The synthesis method (and pretreatment), atoms coordination, specific surface area, temperatures of isopropanol chemisorption, number of surface and/or bulk active acid sites (Ns) and temperature of propylene desorption of bulk WO_3, Wells–Dawson and Keggin HPAs along with monolayer supported and nano-structured tungsten based materials (30%WO_3/ZrO_2) are presented in Table 1.

Isopropanol adsorption was performed at several temperatures in order to determine the more suitable conditions for the alcohol chemisorption on the active sites avoiding further reaction. The observation that no molecular isopropanol is detected in the TPSR spectra indicates that no physisorption (or weak chemisorption) of the alcohol is produced even at 313 K over heteropolyacids (spectra not shown). The maximum amount of surface isopropoxy species over tungsten oxide WO_3 and monolayer supported tungsten oxide species was obtained through isopropanol adsorption at 383 and 343 K, respectively.

The number of available surface sites for isopropanol adsorption of bulk tungsten trioxide and monolayer supported tungsten oxide catalysts, even mesoporous nanoparticles, is orders of magnitude (0.9–6 μmol/m^2) lower than bulk heteropolyacids (8–55 μmol/m^2). This observation can not be attributed to the surface structure since all these materials possess polymerized WO_6 species with octahedral coordination (see Table 1). Moreover, no correlation is observed with the specific surface area since high surface area, mesoporous monolayer supported catalysts possess lower Ns than bulk HPAs.

This observation evidences that the adsorption of alcohol occurs exclusively at the outermost surface layer of WO_3 and monolayer supported tungsten oxide catalysts. However, the characteristic pseudoliquid behavior of the heteropolyacids allows the adsorption of alcohol on the external surface and within the bulk structure. This phenomenon accounts for the high Ns of these solids compared with monolayer supported catalysts. The abnormally high Ns of the fosfo-molybdic Wells–Dawson acid is attributed to the presence of ethanol derived species modifying the secondary structure of the HPA. In fact, previous investigations demonstrated that the number of accessible surface acid sites is directly influenced by the hydration water since fully hydrated fosfo-tungstic Wells–Dawson acid produces twice the amount of propylene (52 μmol/g) than the anhydrous acid (25 μmol/g) [15]. Moreover a continuous drop of the amount of propylene was observed with the decrease of the degree of hydration of the Wells–Dawson structure. This observation evidences that the loss of water leads to the shortening of the distance between the $P_2W_{18}O_{62}{}^{6-}$ Wells–Dawson units and the decrease of the available active sites for isopropanol chemisorption [18]. On line with these observations, the TPD analysis of the fosfo-molybdic Wells–Dawson acid showed that ethanol is strongly

Table 1
Synthesis methodology, structure, surface area, temperature of isopropanol chemisorption, maximum number of active sites, temperature of propylene desorption (T_p) and activation energy of the surface reaction of tungsten and molybdenum based bulk and supported catalysts

Catalyst	Synthesis	Structure	S_{BET} (m^2/g)	Temperature of adsorption (K)	N_s ($\mu mol/m^2$)	T_p (K)	E_a (kcal/mol)
WO_3	Thermal decomposition	Octahedral	1.3	383	0.9	429	29.1
8% WO_3/TiO_2	Incipient wetness	Octahedral[a]	46.7	343	1.0	429	29.1
6% WO_3/ZrO_2	Incipient wetness	Octahedral[a]	33.8	343	0.2	467	31.7
30% WO_3/ZrO_2	Precipitation w/template	Octahedral	45.8	343	6.4	439	29.8
$H_3PW_{12}O_{40}$	Commercial	Octahedral[b]	5.3	313	19.8	385	26.0
$H_3PMo_{12}O_{40}$	Commercial	Octahedral[b]	15.5	313	3.7	372	25.7
$H_6P_2W_{18}O_{62}$	Organic	Octahedral	3.7	313	8.1	369	24.9
$H_6P_2W_{18}O_{62}$	Ion-exchange (not calcined)	Octahedral	1.1	–	–	–	–
	Ion-exchange (calcined)	Octahedral	1.4	313	10.1	372	25.1
$H_6P_2Mo_{18}O_{62}$	Ion-exchange (not calcined)	Octahedral	2.5	313	54.5	373	25.2
14% P_2W_{18}/ZrO_2	Incipient wetness	Unknown	41.1	343	5.2	384	25.9
15% P_2W_{18}/TiO_2	Incipient wetness	Unknown	40.0	343	3.1	379	25.7
9% P_2W_{18}/SiO_2	Incipient wetness	Unknown	277.3	343	1.5	369	25.1

[a] From Ref. [19].

[b] From Ref. [5].

retained into the structure since desorbs as COx above 673 K. Therefore the HPA still possesses those species after calcination at 373 K and further isopropanol chemisorption. The effect of the organic media as a template of the porous structure is observed also on the fosfo-tungstic Wells–Dawson HPA synthesized through ion-exchange in ethanol media and further calcined. In fact, the acid possesses 64% of total pore volume due to microporous volume after calcination at 673 K, compared with 4% before ethanol desorption. This observation might explain why the calcined acid possesses 20% more available active acid sites (10.1 $\mu mol/m^2$) than the acid synthesized through the conventional organic procedure (8.1 $\mu mol/m^2$) (see Table 1).

3.3.2. Strength of the active acid sites: activation energy for surface species reaction

Previous studies by Wachs et al. demonstrated that the information obtained during the temperature programmed surface reaction of adsorbed intermediate species over powdered samples enables to determine kinetic parameters such as, the activation energy E_a of a surface reaction [20]. The authors demonstrated that the Redhead equation allows determining the activation energy E_a,

$$\frac{E_a}{RT_p^2} = \frac{n}{B}\exp\left(-\frac{E_a}{RT_p}\right)$$

where R is the gas phase constant, B the heating rate, T_p the temperature of desorption (°K) of the surface species and ν is the first-order Arrhenius rate constant pre-exponential factor ($\sim 10^{13}\ s^{-1}$).

This equation was applied to calculate the activation energy for the dehydration of isopropoxy species towards propylene as a measurement of the acid strength of the catalytic materials discussed in the previous section (see Table 1).

The higher activation energy (~29 kcal/mol) of surface reaction over bulk tungsten trioxide and monolayer supported tungsten oxide catalysts than HPAs (~25 kcal/mol) is attributed to the differences in the nature of the active acid sites of those catalysts. Spectroscopic studies of dehydrated monolayer supported tungsten oxide catalysts demonstrated that the surface structure is composed by polymerized octahedrally coordinated WO_x species possessing W=O (mono–oxo) terminal bond and bridging W–O–S (S = tungsten or support cation) bonds. Adsorption of NH_3 and pyridine bases also demonstrated that monolayer supported metal oxide catalysts (Re, Cr, Mo, W, V, Nb, etc.) possess mainly Lewis acid sites and Brönsted sites as a minor contribution [21].

The structure of Wells–Dawson and Keggin type heteropolyacids is composed by a central phosphorous atom PO_4 surrounded by a cage of tungsten atoms. Similarly to monolayer supported tungsten oxide catalysts, each tungsten atom composes WO_6 octahedral units with one terminal double bonded oxygen that are linked together through W–O–W bonds. However, many studies demonstrated that solid HPAs possess stronger Brönsted acids than conventional solid acids in agreement with the evidences obtained in the present investigation [22].

Previous studies by Briand et al. demonstrated that the electronegativity of the oxide support (ZrO_2, Al_2O_3, SiO_2 and TiO_2) influences the catalytic activity of monolayer supported WO_x, VO_x and MoO_x species over oxide supports [23–25]. The oxide support influences the M-O-Support (M = vanadium, molybdenum, tungsten) bond varying the electron density of the active surface species. Therefore, the lower the electronegativity of the metal cation [Zr(IV) < Ti(IV) < Al(III) < Si(IV)] the higher redox activity of the surface active sites towards the selective oxidation of methanol to formaldehyde.

On line with those observations, the influence of the electronegativity of the central phosphorous atom on the P–O–W and P–O–Mo bonds and the nature of oxide supports on the acidity of the HPAs were investigated. Fig. 6 compares the activation energy of isopropanol surface reaction towards propylene of bulk and supported HPAs along with monolayer

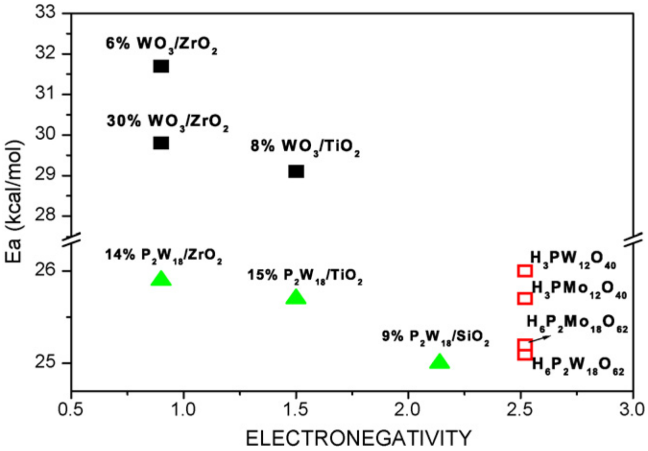

Fig. 6. Activation energy of the surface reaction of chemisorbed isopropoxy species towards propylene over monolayer supported tungsten species, bulk and supported heteropolyacids.

supported tungsten species on oxide supports versus the Sanderson electronegativity of P(V), Si(IV), Ti(IV) and Zr(IV).

Monolayer supported tungsten species on oxide supports (6% WO$_3$/ZrO$_2$, 30% WO$_3$/ZrO$_2$ and 8% WO$_3$/TiO$_2$) were used as model catalysts in order to demonstrate that the activation energy of isopropanol reaction E_a is suitable to be used as a tool to evidence the effect of the nature of the oxide support on the surface reaction. In fact, the activation energy is higher the lower the electronegativity of the oxide support indicating that the acid strength of the surface tungsten species is influenced due to the interaction with the oxide support.

The HPAs possess phosphorous as the central atom, which might explain the observation that they possess similar values of activation energy. Moreover, the dispersion of the fosfo-tungstic Wells–Dawson acid over SiO$_2$ does not modify the activation energy. However, the dispersion of the acid over ZrO$_2$ of lower electronegativity than SiO$_2$, rises the activation energy about 1 kcal. This evidence suggests that an electronic deficiency of the surface active sites improves their acid strength.

4. Conclusions

The present investigation demonstrates that the ion-exchange methodology is a reliable method for the synthesis of fosfo-tungstic and molybdic Wells–Dawson acids in a higher yield than the conventional organic route.

The chemisorption of isopropanol at 313 K leads to the coverage of the catalysts with a monolayer of adsorbed isopropoxy species and avoids surface reaction. Heteropolycompounds are highly active towards isopropanol dehydration above that temperature. Temperature programmed reaction analysis leads to the decomposition of adsorbed isopropoxy species towards propylene at about 373 K. The temperature of desorption allows the calculation of the activation energy of the surface reaction and the comparison of the properties of the active sites.

The number of available acid sites of Keggin and Wells–Dawson heteropolyacids is significantly higher than bulk WO$_3$ and even monolayer supported tungsten oxide species. This observation evidences that the alcohol is adsorbed both on the surface and the bulk in agreement with the pseudo-liquid phase behavior of the heteropolyanion structure. Moreover, the activation energy of surface decomposition of adsorbed isopropoxy species towards propylene is significantly lower on the heteropolyacids rather than the other tungsten oxide based catalysts. The higher acid strength of the HPAs than WO$_3$ and monolayer supported tungsten oxide catalysts is attributed to the presence of Brönsted acid sites and the electronic deficiency caused by the highly electronegative central phosphorous atom.

Acknowledgements

The authors acknowledge Will Knowls for the nanostructured tungsten–zirconia sample and the financial support provided by Agencia Nacional de Promoción Científica y Tecnológica (PICT 14-12161/02) and Universidad Nacional de La Plata (project 11-X 378).

References

[1] N. Mizuno, M. Misono, Chem. Rev. 98 (1998) 1999.
[2] T. Okuhara, N. Mizuno, M. Misono, Adv. Catal. 41 (1996) 113.
[3] L.E. Briand, G.T. Baronetti, H.J. Thomas, Appl. Catal. 256 (2003) 37.
[4] P. Vázquez, L. Pizzio, C. Cáceres, M. Blanco, H. Thomas, E. Alesso, L. Finkielsztein, B. Lantaño, G. Moltrasio, J. Aguirre, J. Mol. Catal. A: Chem. 161 (2000) 223.
[5] M.T. Pope, Heteropoly and Isopoly Oxometalates, Springer-Verlag, Berlin, 1983.
[6] H. Wu, J. Biol. Chem. 43 (1920) 189.
[7] G.M. Maksimov, R.I. Maksimovskaya, I.V. Kozhevnikov, Russ. J. Ind. Chem. 39 (1994) 595.
[8] T.P. Wijesekera, J.E. Lyons, P.E. Ellis, Jr., US 6,060,419, May 9, 2000.
[9] T.P. Wijesekera, J.E. Lyons, P.E. Ellis, Jr., US 6,169,202, January 2, 2001.
[10] L.E. Briand, G.M. Valle, H.J. Thomas, J. Mater. Chem. 12 (2002) 299.
[11] M. Filowitz, R.K.C. Ho, W.G. Klemperer, W. Shum, Inorg. Chem. 18 (1979) 93.
[12] G. Baronetti, L. Briand, U. Sedran, H. Thomas, Appl. Catal. 172 (1998) 265.
[13] D.S. Kim, M. Ostromecki, I.E. Wachs, J. Mol. Catal. A: Gen. 106 (1996) 93.
[14] M.S. Wong, E.S. Jeng, J.Y. Ying, Nano Lett. 1 (2001) 637.
[15] L.A. Gambaro, L.E. Briand, Appl. Catal. 264 (2004) 151.
[16] G.M. Valle, L.E. Briand, Mater. Lett. 57 (2003) 3964.
[17] A. Concellón, P. Vázquez, M. Blanco, C. Cáceres, J. Colloids Int. Sci. 204 (1998) 256.
[18] J.E. Sambeth, G.T. Baronetti, H.J. Thomas, J. Mol. Catal. A: Chem. 191 (2003) 35.
[19] H. Hu, I.E. Wachs, S. Bare, J. Phys. Chem. 99 (1995) 10897.
[20] I.E. Wachs, J.-M. Jehng, W. Ueda, J. Phys. Chem. B 109 (2005) 2275.
[21] I.E. Wachs, Colloids Surf. 105 (1995) 143.
[22] T. Okuhara, N. Mizuno, M. Misono, in: D.D. Eley, W.O. Haag, B. Gates (Eds.), Catalytic Chemistry of Heteropoly Compounds, vol. 41, Academic Press Inc., Adv. Catal., 1996. p. 113.
[23] L.G. Burcham, L.E. Briand, I.E. Wachs, Langmuir 17 (2001) 6164.
[24] L.G. Burcham, L.E. Briand, I.E. Wachs, Langmuir 17 (2001) 6175.
[25] L.E. Briand, W.E. Farneth, I.E. Wachs, Catal. Today 62 (2000) 219.